Int. J. Heat Mass Transfer. Vol. 16, pp. 2355–2367. Pergamon Press 1973. Printed in Great Britain

VORTEX INSTABILITY OF NATURAL CONVECTION FLOW ON INCLINED SURFACES

S. E. HAALAND and E. M. SPARROW
Fluid Mechanics Program, University of Minnesota, Minneapolis, Minnesota, U.S.A.

(*Received* 10 *January* 1973 *and in revised form* 25 *May* 1973)

Abstract—The linear stability of laminar natural convection flow adjacent to a heated, inclined, upward-facing plate is investigated for disturbances having the form of longitudinal vortices. The stability problem is formulated with account being taken of the fact that the basic flow and temperature fields depend on the streamwise coordinate. One of the demonstrated consequences of retaining the transverse velocity of the basic flow is the so-called bottling effect, wherein the disturbance vorticity and temperature are contained within the respective boundary layers of the basic flow. The calculated neutral stability curves exhibit an altogether different character depending upon whether the streamwise dependence of the basic flow and temperature fields is taken into account or suppressed; the magnitude of the critical Grashof numbers from the two models differs by several orders of magnitude. The results also show that the greater the inclination of the plate from the vertical, the more susceptible is the flow to the vortex-type instability. The relationship of the analytical results to available experimental information is discussed.

INTRODUCTION

RECENT flow visualization experiments [1] on natural convection adjacent to a heated, inclined, upward-facing plate revealed that a secondary flow in the form of longitudinal vortices may occur owing to the instability of the basic two-dimensional laminar flow. The instability mechanism for such a secondary flow is the presence of a buoyancy force component in the direction normal to the plate surface. Earlier, Görtler [2] and Kirchgässner [3] had identified the normal component of the buoyancy force as being responsible for the secondary-flow vortices adjacent to a heated, horizontal or slightly inclined, upward-facing plate situated in a forced convection flow.

In this paper, the linear stability of laminar natural convection flow on a heated inclined plate is investigated for disturbances having the form of longitudinal vortices. The paper is drawn from the thesis of Haaland [4], which was concerned with the stability of the general class of flows where (a) the streamwise velocity vanishes in the free stream, and (b) the transverse velocity is inward directed and has a finite value in the free stream. The natural convection flow on an inclined plate is a member of this class, which will hereafter be referred to as Class A flows.

For Class A flows, the assumption that the basic flow can be treated as a parallel flow, which is the cornerstone of conventional linear stability theory, is not uniformly valid throughout the entire domain. In particular, the convection of disturbance quantities by the transverse velocity of the basic flow cannot be neglected. As will be demonstrated later for the inclined plate, the retention of the parallel flow assumption leads to significant errors in the stability results.

The aforementioned transverse convection terms give rise to the so-called bottling effect, whereby the disturbance vorticity and temperature are contained (i.e. bottled in) within the boundary layer of the basic flow. Owing to this containment, any Class A stability problem (including the inclined plate) which was previously defined on an unbounded domain can now be defined on a bounded domain.

In addition to accounting for the transverse

velocity of the basic flow, all other terms which arise directly from the x-dependence of the basic flow also will be included in the analysis. The latter terms are taken into account because their importance increases as the wave number—Reynolds number product becomes smaller.

The disturbance equations are formulated in such a manner as to make them independent of the inclination angle of the plate. Subsequent to the demonstration of the bottling effect, neutral stability characteristics are determined for Prandtl numbers of 0·733, 2 and 6·7 by employing a combined analytical–numerical solution method. These Prandtl numbers cover the range of gases, vapors, and liquid water. The thus-obtained stability results are compared with those based on the conventional parallel flow model. Comparisons are made with experiment whenever possible.

THE DISTURBANCE EQUATIONS

The starting point for the derivation of the disturbance equations is the Boussinesq form of the conservation laws (e.g. Landau and Lifshitz [5]).

$$\frac{\partial \boldsymbol{V}}{\partial t} + \boldsymbol{V}.\nabla \boldsymbol{V} = -\frac{1}{\rho}\nabla p - \boldsymbol{g}\beta(T - T_\infty) + \nu\nabla^2 \boldsymbol{V}, \quad (1)$$

$$\nabla . \boldsymbol{V} = 0, \quad (2)$$

$$\frac{\partial T}{\partial t} + \boldsymbol{V}.\nabla T = a\nabla^2 T, \quad (3)$$

where $\boldsymbol{V}$ is the velocity vector, p the reduced pressure (static pressure minus hydrostatic pressure), $\boldsymbol{g}$ the gravity vector, T the temperature, and T_∞ the ambient temperature. The fluid properties, density ρ, thermal expansion coefficient β, kinematic viscosity ν, and thermal diffusivity a are assumed to be constant. The derivation will follow that of Haaland [4].

If one takes the curl of equation (1), there is obtained after using the continuity equation (2) and introducing the vorticity $\boldsymbol{\Omega} = \nabla \times \boldsymbol{V}$

$$\frac{\partial \boldsymbol{\Omega}}{\partial t} + \boldsymbol{V}.\nabla \boldsymbol{\Omega} - \boldsymbol{\Omega}.\nabla \boldsymbol{V} = \beta \boldsymbol{g} \times \nabla T + \nu\nabla^2 \boldsymbol{\Omega}. \quad (4)$$

In a coordinate system where x is the streamwise direction (along the plate), y is in the transverse direction (normal to the plate), and z is in the spanwise direction, $\boldsymbol{V} = (\hat{U}, \hat{V}, \hat{W})$, $\boldsymbol{\Omega} = (\hat{\Omega}_x, \hat{\Omega}_y, \hat{\Omega}_z)$, $T = \hat{T}$, and $\boldsymbol{g} = (g_x, g_y, 0)$. With these, the x-component of the vorticity equation (4) becomes

$$\frac{\partial \hat{\Omega}_x}{\partial t} + \hat{U}\frac{\partial \hat{\Omega}_x}{\partial x} + \hat{V}\frac{\partial \hat{\Omega}_x}{\partial y} + \hat{W}\frac{\partial \hat{\Omega}_x}{\partial z} - \left(\hat{\Omega}_x \frac{\partial \hat{U}}{\partial x} + \hat{\Omega}_y \frac{\partial \hat{U}}{\partial y} + \hat{\Omega}_z \frac{\partial \hat{U}}{\partial z}\right) = \beta g_y \frac{\partial T}{\partial z} + \nu\nabla^2 \hat{\Omega}_x. \quad (5)$$

The basic flow is a two-dimensional boundary layer flow which depends on x and y and is denoted by $(U, V, 0)$, $(0, 0, \Omega)$, and T. The disturbance flow will be characterized by (u, v, w), $(\omega, \omega_y, \omega_z)$, p and τ. The disturbances are assumed to be non-oscillatory in x. Furthermore, if amplified disturbances are assumed to grow in the x-direction, then an operational criterion for neutral stability is that the first derivative of all disturbance quantities with respect to x are zero. In addition, it will be assumed that the second-order derivatives of the disturbances with respect to x are small in the vicinity of the neutral curve, so that the boundary layer assumption can be used whereby $\partial^2/\partial x^2$ is neglected compared with $\partial^2/\partial y^2$. In view of the foregoing and confining attention to neutral stability, the disturbances are taken to be independent of x.* Furthermore, it is known as an experimental fact that the secondary flow vortices (e.g. Görtler vortices) are unchanging with time and periodic in the spanwise coordinate z. Consequently, the disturbance flow will be taken as a function of y and z.

Introducing the sum of the basic flow and the disturbance flow into equation (5), subtracting out the basic flow vorticity equation, and

* If stability characteristics away from the neutral curve were to be sought, then the x-dependence (and, therefore, the x-derivatives) of the disturbances would somehow have to be taken into account.

neglecting nonlinear terms in the disturbances, we get

$$V\frac{\partial\omega}{\partial y} - \Omega\frac{\partial u}{\partial z} - \omega\frac{\partial U}{\partial x} - \omega_y\frac{\partial U}{\partial y} = \beta g_y\frac{\partial\tau}{\partial z} + \nu\nabla^2\omega, \quad (6)$$

where, in equation (6) and thereafter, ∇^2 is the Laplace operator in y and z. Consistent with the boundary layer model for the basic flow, $\Omega = -\partial U/\partial y$. Also, $\omega_y = \partial u/\partial z$ since $\partial w/\partial x = 0$. With these substitutions, equation (6) reduces to

$$V\frac{\partial\omega}{\partial y} + \omega\frac{\partial V}{\partial y} = \beta g_y\frac{\partial\tau}{\partial z} + \nu\nabla^2\omega, \quad (7)$$

which is a differential equation connecting the disturbance vorticity component ω and the disturbance temperature τ.

Inasmuch as $\partial u/\partial x = 0$, the disturbance velocity components v and w may be expressed in terms of a stream function ψ by $v = -\partial\psi/\partial z$, $w = \partial\psi/\partial y$. Consequently,

$$\omega = \frac{\partial w}{\partial y} - \frac{\partial v}{\partial z} = \frac{\partial^2\psi}{\partial y^2} + \frac{\partial^2\psi}{\partial z^2}. \quad (8)$$

The disturbance energy equation is deduced from (3) as

$$u\frac{\partial T}{\partial x} + V\frac{\partial\tau}{\partial y} - \frac{\partial\psi}{\partial z}\frac{\partial T}{\partial y} = a\nabla^2\tau, \quad (9)$$

where account has been taken of $\partial\tau/\partial x = 0$. The u component is brought into the problem via the x-momentum equation for the disturbance

$$-u\frac{\partial V}{\partial y} + V\frac{\partial u}{\partial y} - \frac{\partial\psi}{\partial z}\frac{\partial U}{\partial y} = -\beta g_x\tau + \nu\nabla^2 u \quad (10)$$

in the derivation of which it has been noted that $\partial p/\partial x = \partial u/\partial x = 0$.

Equations (7)–(10) constitute a coupled system for the four disturbance quantities ψ, ω, u and τ. All terms arising from the x-dependence of the basic flow and temperature fields have been retained.

If the inclination of the plate is defined by the acute angle θ between the plate surface and the vertical, then

$$g_x = -g\cos\theta, \quad g_y = -g\sin\theta, \quad (11)$$

where g is the magnitude of the gravity vector. By employing equation (11), the gravity components g_x and g_y can be eliminated from equations (7) and (10).

The disturbance field is periodic in the spanwise coordinate z. Furthermore, as previously discussed, the x-dependences have been neglected at the neutral curve. Consequently, the disturbance quantities ψ, ω, τ, u that appear in equations (7)–(10) are assumed to be locally of the form

$$\psi = \phi(y)\sin\alpha z, \quad \omega = \omega(y)\sin\alpha z, \quad (12a)$$

$$\tau = \tau(y)\cos\alpha z, \quad u = u(y)\cos\alpha z. \quad (12b)$$

The quantity α is the wave number of the disturbance.

Equations (12a) and (12b) are then substituted into equations (7)–(10) and the indicated operations performed. Before stating the outcome, dimensionless variables and parameters will be introduced along with the basic flow and temperature solutions. The scales for the nondimensionalization are motivated by an examination of the form of the basic flow solution.

With respect to the basic flow, it is relevant first to discuss the influence of the buoyancy force in the direction normal to the plate surface. As shown in the Appendix, this buoyancy force induces a streamwise pressure gradient whose magnitude is of the order of $(\tan\theta)/R$ relative to the streamwise buoyancy force (R is a characteristic Reynolds number). In addition, the analysis of Kierkus [6] has demonstrated that for vertical and inclined plates, the boundary layer displacement effect

is of the order of $1/R$. Consequently, for plate inclination angles for which $\tan\theta \sim 1$ or less, the effects of the induced pressure gradient and the boundary layer displacement are of the same order. Provided that $R \gg 1$, both effects are small and will, therefore, be neglected.

Subject to the foregoing restrictions, the basic flow and temperature solutions can be written in the following form

$$U = U^*(x)\bar{U}(\eta), \quad V = \frac{U^*(x)}{R(x)}\bar{V}(\eta),$$
$$T = T_\infty + (T_w - T_\infty)\bar{T}(\eta), \tag{13}$$

where

$$\eta = y/h(x), \quad R = U^*h/\nu, \tag{14}$$

and

$$Gr = \beta g\cos\theta(T_w - T_\infty)x^3/\nu^2 = R^4/64. \tag{15}$$

The specific expressions for U^*, $\bar{U}$, ... are given in the Appendix, equations (A.7)–(A.9). In the foregoing, η can be identified as a similarity variable based on the characteristic length h (proportional to the boundary layer thickness), whereas R is a Reynolds number based on h and on the characteristic velocity U^*. The relationship between the Reynolds number R and the Grashof number is expressed by equation (15). Wherever gravity enters the basic flow solution, it is always as $g\cos\theta$. The quantity T_w is the plate surface temperature.

By making use of the scales U^*, h, and $(T_w - T_\infty)$ suggested by the basic flow and temperature solutions, the amplitudes of the disturbance quantities can be recast into non-dimensional forms as

$$\tilde{\phi}(\eta) = \frac{\phi}{U^*h}, \quad \tilde{\omega}(\eta) = \frac{\omega}{(U^*/h)}, \quad \tilde{\tau}(\eta)$$
$$= \frac{\tau}{T_w - T_\infty}, \quad \tilde{u}(\eta) = \frac{u}{U^*}. \tag{16}$$

In addition, the wave number may be made dimensionless with respect to the length scale h

$$\tilde{\alpha} = \alpha h. \tag{17}$$

Then, upon introducing equations (12) into the disturbance equations (7)–(10) and subsequently employing (13), (14), (16) and (17), one has, after dropping the tilde

$$\phi'' - \alpha^2\phi = \omega, \tag{18}$$

$$\omega'' - \alpha^2\omega = -\alpha\tau\tan\theta + (V\omega)', \tag{19}$$

$$\tau'' - \alpha^2\tau = -\alpha PrRT'\phi + Pr(V\tau' - \eta T'u), \tag{20}$$

$$u'' - \alpha^2 u = -\tau - \alpha RU'\phi + Vu' - V'u. \tag{21}$$

where the primes indicate differentiation with respect to η and Pr denotes the Prandtl number. Examination of the system (18)–(21) reveals that the inclination angle θ appears as a parameter. This system can be made independent of θ by employing new variables and parameters defined as

$$\bar{\phi} = \tilde{\phi}, \quad \bar{\omega} = \tilde{\omega}, \quad \bar{\tau} = \tilde{\tau}\tan\theta,$$
$$\bar{u} = \tilde{u}\tan\theta, \quad \bar{R} = R\tan\theta. \tag{22}$$

Then, upon introduction of equation (22) into (18)–(21) and omitting the overbars, the final form of the disturbance equations is obtained

$$\phi'' - \alpha^2\phi = \omega, \tag{23}$$

$$\omega'' - \alpha^2\omega = -\alpha\tau + (V\omega)', \tag{24}$$

$$\tau'' - \alpha^2\tau = -\alpha PrRT'\phi + Pr(V\tau' - \eta T'u), \tag{25}$$

$$u'' - \alpha^2 u = -\tau - \alpha RU'\phi + Vu' - V'u. \tag{26}$$

Equations (23)–(26) contain several terms which would have been neglected had the conventional parallel flow assumption been made. These include $(V\omega)'$ in equation (24), $(Vu' - V'u)$ in equation (26), and $PrV\tau'$ in equation (25). Furthermore, since the parallel flow model implies that the x-dependence of the basic flow and temperature field can be neglected, the term $Pr\eta T'u$ in equation (25) would have been omitted. Inasmuch as this term is the only place where u appears in equations (23)–(25), its omission would enable equation (26) to be deleted altogether from the system.

The boundary conditions that $u, v(= -\partial\psi/\partial z)$, $w(= \partial\psi/\partial y)$, and τ vanish at the plate surface

and in the free stream can be restated as

$$u = \phi = \phi' = \tau = 0 \quad \text{at} \quad \eta = 0 \quad \text{and} \quad \infty. \tag{27}$$

The system (23)–(27) is homogeneous and, therefore, admits a trivial solution. To obtain a non-trivial solution, a normalizing condition is imposed, for instance,

$$\omega(0) = 1. \tag{28}$$

Equations (27) and (28) contain nine conditions for the eighth-order system (23)–(26). Therefore, one of the parameters α, R has to be an eigenvalue. In the present study, R was selected as the eigenvalue and a succession of values was assigned to α, thereby yielding the neutral curve $R = R(\alpha)$.

The solution method to be employed here uses analytical solutions for large η in conjunction with numerical integration for intermediate and small η. The large-η solutions will now be developed and will be subsequently applied in the demonstration of the bottling effect.

LARGE-η SOLUTIONS AND THE BOTTLING EFFECT

As a starting point for the development of a solution of equations (23)–(26) that is valid for large values of η, it is necessary to know the large-η solutions for the basic flow and temperature. From equations (A.12) and (A.13), it follows that for large-η, $F = F_\infty + F_1$ and $H = H_1$, where F_1 and H_1 are the first terms of exponentially decreasing expansions which involve known constants that depend on the Prandtl number. Furthermore, from equation (A.9)

$$U = F_1' \equiv U_1, \tag{29a}$$

$$V = -3F_\infty + (\eta F_1' - 3F_1) \equiv V_\infty + V_1, \tag{29b}$$

$$T = H_1 \equiv T_1. \tag{29c}$$

Large-η solutions for ϕ, ω, τ and u will now be sought in the form of a series of decreasing functions

$$\phi = A_1 + A_2 + \ldots, \quad \omega = B_1 + B_2 + \ldots,$$
$$\tau = C_1 + C_2 + \ldots, \quad u = D_1 + D_2 + \ldots. \tag{30}$$

When equations (29) and (30) are substituted into (23)–(26) and terms of like order are collected, one gets, to the first order

$$LA_1 = B_1, \quad MB_1 = -\alpha C_1, \quad NC_1 = 0, \quad MD_1 = -G_1 \tag{31}$$

and to the second order

$$LA_2 = B_2, \quad MB_2 = -\alpha C_2 + V_1 B_1' + V_1' B_1, \tag{32a}$$

$$NC_2 = -\alpha PrRT_1 A_1 + Pr(V_1 C_1' - \eta T_1 D_1), \tag{32b}$$

$$MD_2 = -C_2 - \alpha R U_1' A_1 + V_1 D_1' - V_1' D_1, \tag{32c}$$

where the operators L, M, N and D are given by

$$L = D^2 - \alpha^2, \quad M = D^2 - V_\infty D - \alpha^2, \tag{33a}$$

$$N = D^2 - V_\infty Pr D - \alpha^2, \quad D = \mathrm{d}/\mathrm{d}\eta. \tag{33b}$$

There are four independent solutions of equations (31) and (32) which vanish at infinity. The solutions are designated by subscripts 1–4. For the first set of solutions

$$\phi_1 = \mathrm{e}^{-\alpha\eta} + \mathrm{e}^{-\alpha\eta} O[\mathrm{e}^{-|V_\infty| Pr\eta}],$$
$$(\omega_1, \tau_1, u_1) = (b_1, b_2, b_3)\mathrm{e}^{-(\alpha + |V_\infty| Pr)\eta}, \tag{34}$$

in which the b_1, b_2 and b_3 are abbreviations for lengthy expressions which contain $|V_\infty|$, Pr, α, R and the known constants G_i of equations (A.12) and (A.13). For the second set of solutions

$$\phi_2 = \mathrm{e}^{-\gamma\eta}/(\gamma |V_\infty|), \quad \omega_2 = \mathrm{e}^{-\gamma\eta},$$
$$\tau_2 \sim \mathrm{e}^{-(\gamma + |V_\infty| Pr)\eta},$$
$$u_2 \sim \max[\mathrm{e}^{-(\gamma + |V_\infty| Pr)\eta}, \ \mathrm{e}^{-(\gamma + |V_\infty|)\eta}]. \tag{35}$$

For the third set of solutions

$$\phi_3 = \frac{-\alpha \mathrm{e}^{-\lambda\eta}}{\lambda^2 |V_\infty|^2 (Pr - 1) Pr},$$

$$\omega_3 = \frac{-\alpha \mathrm{e}^{-\lambda\eta}}{\lambda |V_\infty| (Pr - 1)}, \quad \tau_3 = \mathrm{e}^{-\lambda\eta},$$

$$u_3 = \frac{-\mathrm{e}^{-\lambda\eta}}{\lambda |V_\infty| (Pr - 1)}. \tag{36}$$

For the fourth set of solutions

$$\phi_4 \sim \omega_4 \sim \tau_4 \sim e^{-(\gamma+|V_\infty|Pr)\eta}, \quad u_4 = e^{-\gamma\eta}. \quad (37)$$

The quantities γ and λ that appear in the foregoing are

$$\gamma = |V_\infty|/2 + \sqrt{(V_\infty^2/4 + \alpha^2)},$$
$$\lambda = |V_\infty|Pr/2 + \sqrt{(V_\infty^2 Pr^2/4 + \alpha^2)}. \quad (38)$$

An assessment will now be made of the relative rates at which the disturbance field and the basic flow decay at large η. By employing equations (A.9), (A.12) and (A.13) and noting that $\Omega \sim \partial U/\partial\eta$, one has for the basic flow

$$\Omega, U \sim \max\left[e^{-|V_\infty|\eta}, \quad e^{-|V_\infty|Pr\eta}\right],$$
$$T \sim e^{-|V_\infty|Pr\eta}. \quad (39)$$

The decay rates for the disturbance quantities ω, u and τ are expressed by the just-derived equations (34)–(37). In employing these relations for comparison with (39), it is relevant to note that $\lambda > |V_\infty|Pr$ and $\gamma > |V_\infty|$. The comparison of decay rates has to be made separately for $Pr > 1$ and $Pr < 1$.

When $Pr > 1$, the following ratios can be formed

$$\frac{\omega}{\Omega} \sim \frac{\max\left[e^{-(\alpha+|V_\infty|Pr)\eta}, e^{-\gamma\eta}, e^{-\lambda\eta}, e^{-(\gamma+|V_\infty|Pr)\eta}\right]}{e^{-|V_\infty|\eta}}, \quad (40a)$$

$$\frac{u}{\Omega} \sim \frac{\max\left[e^{-(\alpha+|V_\infty|Pr)\eta}, e^{-(\gamma+|V_\infty|Pr)\eta}, e^{-\lambda\eta}, e^{-\gamma\eta}\right]}{e^{-|V_\infty|\eta}}, \quad (40b)$$

$$\frac{\tau}{T} \sim \frac{\max\left[e^{-(\alpha+|V_\infty|Pr)\eta}, e^{-(\gamma+|V_\infty|Pr)\eta}, e^{-\lambda\eta}\right]}{e^{-|V_\infty|Pr\eta}}. \quad (40c)$$

From an examination of equations (40), it is seen that

$$\frac{\omega}{\Omega}, \quad \frac{u}{\Omega}, \quad \frac{\tau}{T} \to 0 \quad \text{as} \quad \eta \to \infty. \quad (41)$$

Furthermore, it is easily shown that the disturbance vorticity components ω_y and ω_z decay at the same rate as does u; consequently,

$$\frac{\omega_y}{\Omega}, \quad \frac{\omega_z}{\Omega} \to 0 \quad \text{as} \quad \eta \to \infty. \quad (42)$$

When $Pr < 1$, Ω, U, $T \sim \exp(-|V_\infty|Pr\eta)$. By forming ratios similar to equations (40), one finds that the conclusions expressed by equations (41) and (42) continue to be valid. Moreover, since Ω and T decay at similar rates for $Pr < 1$, it follows that $(\omega, \omega_y, \omega_z)/T$ and u/T also approach zero.

Equations (41) and (42) show that the disturbance vorticity decays faster than the basic flow vorticity and that the disturbance temperature decays faster than the basic flow temperature. This means that the disturbance vorticity and temperature fields are contained within the corresponding boundary layers of the basic flow; that is, the disturbance fields are bottled in.

If the transverse velocity terms $V\partial/\partial y(\omega, \tau, u)$ had been omitted from the disturbance equations, as in a conventional parallel flow model, then all disturbances would have decayed as $\exp(-\alpha\eta)$. For small values of α, $\exp(-\alpha\eta)$ decays more slowly than do Ω, U and T, so that the disturbances would not have been bottled in. It follows, therefore, that the inward-directed transverse velocity of the basic flow is responsible for the bottling effect.

METHOD OF SOLUTION

The details of the solution method have been described by Haaland [4], so that only a general outline need be presented here. The solution method involves the use of the large-η analytical solutions for ϕ, ω, τ and u in conjunction with numerical integration at intermediate and small η. The large-η solutions furnish the starting values for the numerical integration of equations (23)–(26), which proceeds inward from some large value of $\eta(=\eta^*)$ toward the plate surface ($\eta = 0$).

It can be seen from equations (34)–(37) that for assigned values of Pr, α and R, the large-η solutions yield numerical values for ϕ, ω, τ, u and their derivatives at $\eta = \eta^*$. With $\phi_1, \omega_1, \tau_1, u_1$

and their derivatives at η^* as starting values, equations (23)–(26) are numerically integrated to $\eta = 0$. A second solution is then obtained by performing the numerical integration using ϕ_2, ω_2, τ_2, u_2 and their derivatives at η^* as the starting values. Similarly, a third and a fourth solution are obtained by starting respectively with $\phi_3, \ldots$ and $\phi_4, \ldots$ at η^*.

The four solutions thus obtained are summed up, with each solution being multiplied by a constant. The constants are determined by employing the normalizing condition $\omega(0) = 1$ along with three of the wall boundary conditions, say, $\phi(0) = \phi'(0) = u(0) = 0$. This leaves one wall boundary condition, $\tau(0) = 0$, which is satisfied only when R is an eigenvalue. The initial guess for R is refined iteratively by applying the Newton–Raphson method to the boundary condition $\tau(0) = f(R)$, until the desired result $f(R) = 0$ is obtained.

DISTURBANCE EQUATIONS FOR PARALLEL FLOW MODEL

For purposes of comparison, it is appropriate to obtain results from a formulation based on the conventional parallel flow model for the basic flow. The terms which would be deleted from the disturbance equations (23)–(26) on the basis of the parallel flow model have already been discussed in the paragraph that follows those equations. If those deletions are made, the disturbance equations become

$$\phi'' - \alpha^2\phi = \omega, \quad \omega'' - \alpha^2\omega = -\alpha\tau,$$
$$\tau'' - \alpha^2\tau = -\alpha PrRT'\phi. \qquad (43)$$

Upon elimination of ω and τ, one obtains

$$(D^2 - \alpha^2)^3\phi = \alpha^2 PrRT'\phi, \qquad (44)$$

with boundary conditions

$$\phi = \phi' = (D^2 - \alpha^2)^2\phi = 0 \quad \text{at} \quad \eta = 0 \text{ and } \infty. \qquad (45)$$

Outside the thermal boundary layer of the basic flow, $T' = 0$. Consequently, the behavior of ϕ at large η can be determined by solving $(D^2 - \alpha^2)^3\phi = 0$. The three solutions of this equation which vanish at infinity are

$$\phi_1 = e^{-\alpha\eta}, \quad \phi_2 = \eta e^{-\alpha\eta}, \quad \phi_3 = \eta^2 e^{-\alpha\eta}. \qquad (46)$$

These large-η solutions are employed to provide starting values at $\eta = \eta^*$ for the numerical integration of equation (44), which proceeds inward from η^* to the wall ($\eta = 0$). The procedure for finding the eigenvalues R is identical to that already discussed in connection with equations (23)–(26).

RESULTS AND DISCUSSION

Neutral stability results for Prandtl numbers of 0·733, 2 and 6·7 were obtained by solving the eigenvalue problem defined by equations (23)–(28). These Prandtl numbers cover the range for gases, vapors, and liquid water. The corresponding neutral stability curves are presented in Fig. 1. The ordinate variable is the dimensionless wave number $\tilde{\alpha} = \alpha h$ and the abscissa variable is $R \tan\theta$. The Reynolds number R and the characteristic length h are defined by equations (14) and (A.7) respectively. In the interest of clarity, the h and R appearing in the ordinate and abscissa have been recast in terms of the familiar Grashof number Gr

$$Gr = \beta g \cos\theta (T_w - T_\infty)x^3/\nu^2, \qquad (47)$$

which contains the streamwise component of gravity $g\cos\theta$. Also appearing in Fig. 1 is a dashed line representing the neutral curve obtained by solving the eigenvalue problem (44)–(45) which corresponds to the parallel flow model for the basic flow. The dashed line is for $Pr = 6{\cdot}7$.

The most striking feature of Fig. 1 is the markedly different nature of the neutral curves which are respectively obtained when the nonparallelism of the basic flow is taken into account or suppressed. In the former case, the neutral curves exhibit both upper and lower branches and a minimum (i.e. critical) value of the Grashof number which occurs at a finite wave number. On the other hand, for the parallel flow model, the neutral curve does not have a

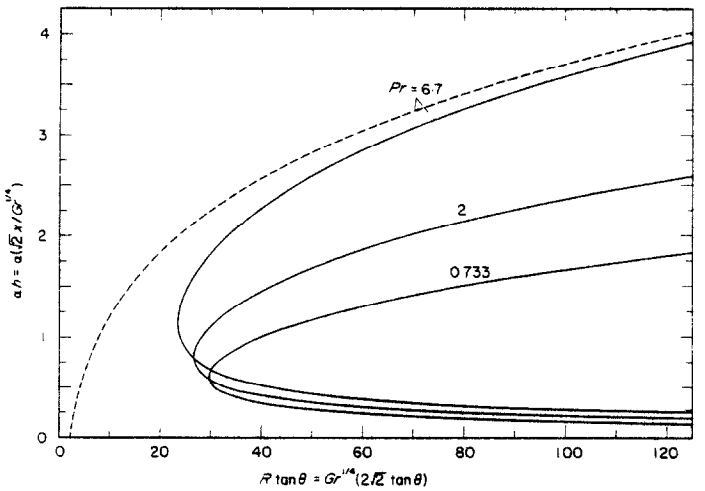

FIG. 1. Neutral stability diagram, dimensionless wave number vs Reynolds number.

lower branch and the minimum Grashof number appears to occur at zero wave number. The magnitude of the minimum Grashof number from the parallel flow model is several orders of magnitude lower than that from the more complete model. Clearly, the accounting of the non-parallel nature of the basic flow has a first-order influence on the neutral stability characteristics.

The influence of the plate inclination angle θ on the stability characteristics can be deduced by examining the solid curves of Fig. 1. If note is taken of the factor $\tan\theta$ which appears in the abscissa variable, it is apparent that the greater the inclination angle, the more susceptible is the flow to the vortex-type instability being investigated here. On the other hand, since $\tan\theta$ approaches zero as θ approaches zero, flows adjacent to plates that are either vertical or nearly vertical are very stable with respect to vortex-type instabilities, and it is highly like that other forms of disturbance (e.g. plane waves) are responsible for the breakdown of laminar flow. These findings are in accord with experiment [7].

The minimum values of $R\tan\theta$ are 23·5, 26·7 and 29·6, respectively for $Pr = 6{\cdot}7$, 2 and 0·733. This is a remarkably small spread, considering the order of magnitude variation in the Prandtl number. By taking the fourth powers of the respective results for $R\tan\theta$ and multiplying by the corresponding Prandtl numbers, it is seen that the Grashof–Prandtl products are by no means constant. Actually, in the range investigated, the numerical values of the critical Grashof number depend less on Prandtl number than do the Grashof–Prandtl products (i.e. Rayleigh numbers).

Whereas a wave number–Reynolds number diagram, such as Fig. 1, is a common vehicle for presenting stability results. it has some major deficiencies. First, the non-dimensional wave number is not, in itself, a measured quantity; rather, it is the wavelength Λ which can be determined from experiment. Second, the streamwise coordinate x appears in both the ordinate and abscissa variables, so that it is difficult to examine how disturbances of given wavelength behave as they move in the streamwise direction.

To facilitate an alternate presentation which avoids these drawbacks, it is convenient to define a characteristic length L^* which is a constant in each particular physical situation

$$L^* = [\beta g \cos\theta(T_w - T_\infty)/\nu^2]^{-\frac{1}{3}}. \quad (48)$$

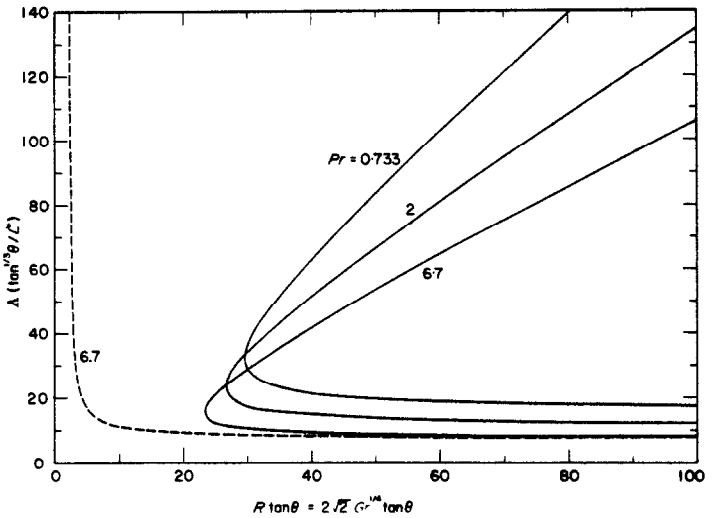

FIG. 2. Neutral stability diagram, wavelength vs Reynolds number

Since $\Lambda = 2\pi/\alpha$, it is easily shown that

$$\frac{\Lambda}{L^*}\tan^{\frac{1}{4}}\theta = \frac{2\pi(R\tan\theta)^{\frac{1}{4}}}{\alpha h}. \qquad (49)$$

With the aid of equation (49), the αh, $R\tan\theta$ diagram (Fig. 1) can be transformed into a diagram of $\Lambda(\tan^{\frac{1}{4}}\theta/L^*)$ vs $R\tan\theta$.

A plot of the neutral stability curves in such a diagram is given in Fig. 2. As before, the neutral curves have an altogether different character depending upon whether the non-parallelism of the basic flow is taken into account or suppressed.

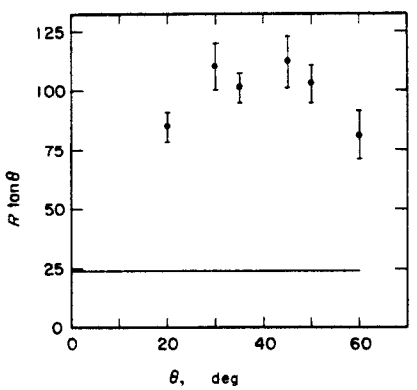

FIG. 3. Vortex instability data of [7], $R\tan\theta$ vs θ.

The experimental instability results of [7] will now be examined. The instability that was investigated resulted from natural disturbances. The experiments were performed using a heated plate situated in water, and instability was identified by the first appearance of vortex lines made visible by an electrochemical reaction. It was not possible to estimate the amount of amplification which might have occurred prior to the first appearance of the lines.

The vortex instability data of the experiments, encompassing six angles of inclination between 20 and 60 degrees, are shown in Fig. 3. For each angle of inclination, the mean value of many repeated readings is indicated along with the corresponding standard deviation. The mean values of $R\tan\theta$ ranged from 80 to 109. On the other hand, from the analytical results (Figs. 1 or 2), the value of $R\tan\theta$ at the critical point is about 24 for the mean Prandtl number of about 5·5 encountered in the experiments. The critical value of $R\tan\theta$ is substantially lower (by a factor of about four) than that marking detectable instability in the experiments of [7]. This is in accord with all known results for *natural disturbances* in boundary layer flows, where appreciable amplification is necessary before

any disturbances can be detected (e.g. [8], p. 507). Due to the scatter of the points in Fig. 3, no clear conclusion can be made about the validity of using $R \tan \theta$ as a correlating parameter for the onset of instability.

There is no information given in [7] about the wavelengths of the observed vortex lines. Fragmentary information is reported in [1], from which the present authors have calculated three values of $\Lambda(\tan^{\frac{1}{4}} \theta/L^*)$, namely 18, 19 and 24. From Fig. 2, the value of $\Lambda(\tan^{\frac{1}{4}} \theta/L^*)$ lies in the range 17–18 for the Prandtl numbers of the experiment. This level of agreement between the critical wavelength and the experimentally observed wavelength is surprisingly good, especially in view of prior lack of agreement for other naturally disturbed boundary layer flows [8–10].

Sufficient data are not available to fully affirm the validity of the correlation $\Lambda(\tan^{\frac{1}{4}} \theta/L^*)$ = constant at the onset of instability. If the correlation holds, then $\Lambda \sim \sin^{-\frac{1}{4}} \theta$ and $\Lambda \sim (\Delta T)^{-\frac{1}{4}}$. The examination of these dependencies of Λ on θ and on ΔT awaits further experiments.

Finally, one last observation will be made. In Fig. 4, the mean values of R from [7] are plotted as a function of the inclination angle θ. At inclinations of -10, 0 and 10 degrees, the observed instability was of the travelling wave type, whereas for larger angles, vortex instability was observed. It is seen that the points fall very nearly on a straight line. The fact that the data from both types of instability lie on a continuous straight line raises the possibility that the two instability types may coexist for a substantial range of angles. It remains for future experiments involving hot-wire equipment to examine the just-discussed possible coexistence. A simple empirical formula for the observed onset of instability can be given as $R = 330 - 4{\cdot}85\,\theta$ for $Pr = 5{\cdot}5$. Also shown in the figure is a line $R \tan \theta = 24$, which represents the critical Reynolds number for a Prandtl number of 5·5. The angular dependence of the critical Reynolds number curve is, evidently, very different from that of the experimental data.

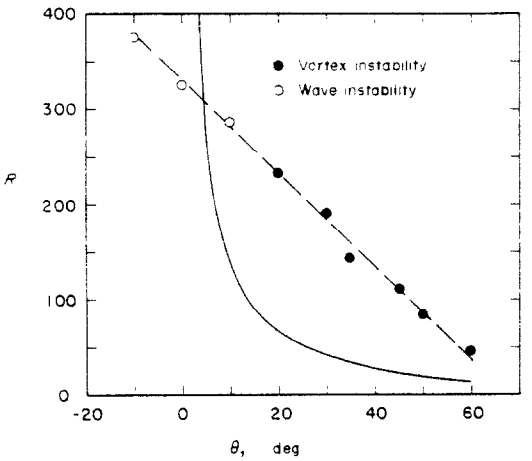

FIG. 4. Instability data of [7]. R vs θ.

CONCLUDING REMARKS

There is a certain similarity between the present problem and the problem of forced flow on curved plates, first treated by Görtler [11]. In the latter problem, the disturbances are in the form of Tollmien–Schlichting waves for zero and small values of the curvature. For larger values of positive curvature (concave plate), the disturbances observed are no longer in the form of travelling waves but are in the form of steady longitudinal vortices (Görtler vortices). The instability in the latter case is due to the centrifugal force normal to the plate, which can be regarded as a body force.

For the Görtler problem, Hämmerlin [12], correcting the calculation of Görtler, also obtained a minimum value of the stability parameter (Görtler number) at a zero wave number. In a later paper [13], he found that the minimum Görtler number occurs at a non-zero wave number when a term connected with the curvature is included. This term was neglected at first because it is small in comparison with another term inside the boundary layer. However, in the outer portion of the boundary layer and outside the boundary layer, this was no longer true. Therefore, the neglect of this term was not uniformly valid throughout the entire domain of the problem. Hämmerlin's finding is

another example of a non-uniform approximation whose impact is more and more strongly felt as the wave number approaches zero. See also [14] for further comments on this approximation.

A question might arise as to the possibility of using linear stability theory to predict a critical angle (or range of angles) at which the disturbances change their character from travelling waves to longitudinal vortices as suggested by the experiments in [7]. Presumably, if one can obtain the value of R for the onset of instability as a function of angle of inclination for both types of disturbances, then one might assume that for any angle the disturbance with the lowest R value would be the one observed. However, as discussed above, in the case of natural disturbances there appears to be no correlation between the observed onset of instability and the critical R value of the neutral curve. Thus, the critical Reynolds number cannot be used for prediction of observed instability. If amplification curves were to be obtained, one could find the range of wavelengths that are amplified most strongly. However, there still is no rational way of deciding at which value of Reynolds number one might expect to observe instability in the presence of natural disturbances. Therefore, it seems improbable that the critical angle can be predicted theoretically, at least by treating each type of disturbance separately. A more promising approach to achieving such a prediction would be to treat the case in which the disturbances contain both longitudinal vortices and travelling waves.

REFERENCES

1. E. M. Sparrow and R. B. Husar, Longitudinal vortices in natural convection flow on inclined surfaces, *J. Fluid Mech.* **37**, 251–255 (1969).
2. H. Görtler, Über eine Analogie zwischen den Instabilitäten laminarer Grenzschichtströmungen an konkaven Wänden und an erwärmten Wänden, *Ing. Arch.* **28**, 71–78 (1959).
3. K. Kirchgässner, Einige Beispiele zur Stabilitätstheorie von Strömungen an konkaven und erwärmten Wänden, *Ing. Arch.* **31**, 115–124 (1962).
4. S. Haaland, Contributions to linear stability theory of nearly parallel flows, Ph.D. thesis in Fluid Mechanics, University of Minnesota, Minneapolis, Minnesota (1972).
5. L. D. Landau and E. M. Lifshitz, *Fluid Mechanics*. Pergamon, Oxford (1959).
6. W. T. Kierkus, An analysis of laminar free convection flow and heat transfer about an inclined isothermal plate, *Int. J. Heat Mass Transfer* **11**, 241–253 (1968).
7. J. R. Lloyd and E. M. Sparrow, On the instability of natural convection flow on inclined plates, *J. Fluid Mech.* **42**, 465–470 (1970).
8. H. Schlichting, *Boundary Layer Theory*. McGraw-Hill, New York (1968).
9. I. Tani, Production of longitudinal vortices in the boundary layer along a concave wall, *J. Geophys. Res.* **67**, 3075–3080 (1962).
10. B. Gebhart, Natural convection flow, instability and transition, *J. Heat Transfer* **91**, 293–309 (1969).
11. H. Görtler, Über eine dreidimensionale Instabilität laminarer Grenzschichten an konkaven Wänden, *Nachr. Ges. Wiss. Göttingen, Fachgr. I (N.F.)* **2**, 1–26 (1940).
12. G. Hämmerlin, Über das Eigenwertproblem der dreidimensionalen Instabilität laminarer Grenzschichten an konkaven Wänden, *J. Rat. Mech. Anal.* **4**, 279–321 (1955).
13. G. Hämmerlin, Zur Theorie der dreidimensionalen Instabilität laminarer Grenzschichten, *ZAMP* **7**, 156–164 (1956).
14. W. L. Witting, Über den Einfluss der Stromlinienkrümmung auf die Stabilität laminarer Strömungen, *Arch. Rat. Mech. Anal.* **2**, 243–283 (1958).

APPENDIX

The Basic Flow and Temperature Solutions

With the usual boundary layer assumptions, the governing equations for natural convection adjacent to a heated, inclined, upward-facing plate are (e.g. Kierkus [6])

$$\frac{\partial U}{\partial x} + \frac{\partial V}{\partial y} = 0, \tag{A.1}$$

$$U\frac{\partial U}{\partial x} + V\frac{\partial U}{\partial y} = -\frac{1}{\rho}\frac{\partial p}{\partial x} + \beta g \cos\theta(T - T_\infty) + \nu\frac{\partial^2 U}{\partial y^2}, \tag{A.2}$$

$$0 = -\frac{1}{\rho}\frac{\partial p}{\partial y} + \beta g \sin\theta(T - T_\infty), \tag{A.3}$$

$$U\frac{\partial T}{\partial x} + V\frac{\partial T}{\partial y} = a\frac{\partial^2 T}{\partial y^2}, \tag{A.4}$$

where, as noted in connection with equation (1), p is the difference between the static pressure and the hydrostatic pressure ($p = 0$ outside the boundary layer).

With a view toward estimating the magnitude of the pressure gradient $\partial p/\partial x$ in equation (A.2), one can first estimate p from equation (A.3) as

$$\frac{p}{\delta} \sim \rho\beta g \sin\theta(T - T_\infty). \tag{A.5}$$

where δ is the boundary layer thickness. Furthermore, if $\partial p/\partial x \sim p/x$, then

$$\frac{1}{\rho}\frac{\partial p}{\partial x} \sim \frac{\delta}{x}\beta g \sin\theta(T - T_\infty). \tag{A.6}$$

Taking the ratio of this quantity to the buoyancy force in equation (A.2) yields $(\delta/x)\tan\theta$ and, since $\delta/x \sim 1/Gr^{\frac{1}{4}} \sim 1/R$, the ratio becomes $(\tan\theta)/R$. As long as $\tan\theta \sim 1$ and $R \gg 1$, the pressure gradient term in equation (A.2) can be neglected compared with the buoyancy term.

The similarity solution for the system (A.1), (A.2) with $\partial p/\partial x$ omitted, and (A.4) can be expressed as indicated in equations (13) and (14), where

$$U^*(x) = 4\nu c^2 x^{\frac{1}{2}}, \quad h(x) = x^{\frac{1}{4}}/c, \tag{A.7}$$

$$c = [\beta g \cos\theta(T - T_\infty)/4\nu^2]^{\frac{1}{4}}, \tag{A.8}$$

$$\bar{U}(\eta) = F', \quad \bar{V}(\eta) = (\eta F' - 3F), \quad \bar{T}(\eta) = H. \tag{A.9}$$

The functions $F(\eta)$ and $H(\eta)$ are the solutions of

$$F''' + 3FF'' - 2F'^2 + H = 0, \quad H'' + 3PrFH' = 0. \tag{A.10}$$

$$F(0) = F'(0) = F'(\infty) = H(\infty) = 0, \quad H(0) = 1. \tag{A.11}$$

Equations (A.10) and (A.11) are readily recognized as the familiar governing equations for the vertical plate problem.

There are many numerical solutions of the system (A.10), (A.11) in the literature. A more efficient solution method for such systems was devised by Haaland ([4], Chapter 6), the main feature of which is the replacement of the given boundary conditions at $\eta = \infty$ with *other* boundary conditions at a finite value of η.

Asymptotic solutions for F and H that are valid at large values of η can be developed as follows

$$F(\eta) = F_\infty + G_1 e^{-3F_\infty \eta} + G_2 e^{-3F_\infty Pr\eta}, \tag{A.12}$$

$$H(\eta) = G_3 e^{-3F_\infty Pr\eta}, \tag{A.13}$$

where G_2 and G_3 are related by

$$G_3 = (3PrF_\infty)^3(1 - 1/Pr)G_2. \tag{A.14}$$

The constants F_∞, G_1, G_2 and G_3 were evaluated by employing the numerical solutions of equations (A.10) and (A.11).

INSTABILITE TOURBILLONNAIRE DE LA CONVECTION NATURELLE SUR DES SURFACES INCLINEES

Résumé—On étudie la stabilité linéaire de la convection naturelle laminaire adjacente à une plaque chauffée, inclinée, à face tournée vers le haut, pour des perturbations ayant la forme de tourbillons longitudinaux. Le problème de stabilité est formulé en tenant compte du fait que les champs de l'écoulement principal et de température dépendent des coordonnées.

Une des conséquences démontrées de la conservation de la vitesse transverse de l'écoulement fondamental est l'effet appelé de mise en bouteille, où la vitesse de perturbation et la température sont contenues dans les couches limites respectives de l'écoulement fondamental. Les courbes de stabilité neutre calculées montrent nettement un caractère différencié suivant que la dépendance des champs de l'écoulement de base et de température est prise en compte ou supprimée; les valeurs du nombre de Grashof pour les deux modèles diffèrent de plusieurs ordres de grandeur. Les résultats montrent aussi que plus l'inclinaison de la plaque est grande à partir de la verticale, plus l'écoulement est sensible à l'instabilité de type tourbillonnaire. On discute l'expression analytique des résultats à partir des informations disponibles sur les expériences.

WIRBEL-INSTABILITÄT BEI NATÜRLICHER KONVEKTION AN GENEIGTEN FLÄCHEN

Zusammenfassung—Die lineare Stabilität der laminaren natürlichen Konvektions-Strömung an einer erwärmten, geneigten nach oben gerichteten Heizfläche wird für Strömungen untersucht, die die Form längslaufender Wirbel haben. Das Stabilitätsproblem wird unter Berücksichtigung der Tatsache dargestellt, dass die Grundströmung und das Temperaturfeld von der stromwärts gerichteten Koordinate abhängt. Eine der dargestellten Folgen beim Festhalten der Quergeschwindigkeit der Grundströmung ist der sogenannte Flascheneffekt, wobei Strömungsverwirbelung und Temperatur durch die betreffende Grenzschicht der Grundströmung erfasst werden. Die errechneten Kurven indifferenter Stabilität zeigen grundsätzlich unterschiedliches Verhalten, je nachdem, ob die Abhängigkeit der Grundströmung und der Temperaturfelder in Strömungsrichtung berücksichtigt oder vernachlässigt wird. Der Wert der kritischen Grashof-Zahl beider Modelle differiert um einige Grössenordnungen. Die Ergebnisse zeigen auch, dass mit zunehmender Neigung der Platte gegenüber der Senkrechten die Empfindlichkeit der Strömung hinsichtlich der Wirbel-Instabilität steigt. Der Vergleich der analytischen Resultate mit verfügbaren experimentellen Aussagen wird erörtert.

ВИХРЕВАЯ НЕУСТОЙЧИВОСТЬ ПРИ ЕСТЕСТВЕННОЙ КОНВЕКЦИИ У НАКЛОННЫХ ПОВЕРХНОСТЕЙ

Аннотация—Исследуется линейная устойчивость ламинарного потока при естественной конвекции над нагретой наклонной пластиной в случае возмущений в виде продольных вихрей. Задача устойчивости формулируется с учетом зависимости основного потока и температурного поля от координаты, направленной вдоль течения. Показано, что одним из условий сохранения поперечной скорости основного потока является ситуация, когда вихри возмущения и температура возмущения заключены в соответствующих пограничных слоях основного потока. Расчетные нейтральные кривые устойчивости в целом имеют различный характер в зависимости от того, учитывается или пренебрегается зависимостью основного потока и температурных полей от продольной координаты; величина критических чисел Грасгофа для двух моделей отличается на несколько порядков. Результаты также показывают, что чем больше пластина от клоняется от вертикали, тем более восприимчив поток к вихревой неустойчивости. Приводится сопоставление результатов анализа с имеющимися экспериментальными данными.